Research Square

Preprints are preliminary reports that have not undergone peer review.
They should not be considered conclusive, used to inform clinical practice,
or referenced by the media as validated information.

Biosorption of Cr(III) and Cr(VI) from Synthetic Solutions on NaOH-Modified Peel of Artocarpus nobilis Fruit – Adsorption Equilibrium Studies

A.P.G.M.V. Samaraweera
University of Peradeniya
N. Priyantha
namalpriyantha@pdn.ac.lk
University of Peradeniya
W. S.S. Gunathilake
University of Peradeniya

Research Article

Keywords: Artocarpus nobilis, isotherm, optimization, error functions, linear, non-linear

Posted Date: April 28th, 2025

DOI: https://doi.org/10.21203/rs.3.rs-6086784/v1

License: This work is licensed under a Creative Commons Attribution 4.0 International License.
Read Full License

Additional Declarations: No competing interests reported.

Biosorption of Cr(III) and Cr(VI) from Synthetic Solutions on NaOH-Modified Peel of *Artocarpus nobilis* Fruit – Adsorption Equilibrium Studies

A.P.G.M.V. Samaraweera[1,2], N. Priyantha[2*] and W.S.S. Gunathilake[2]

[1] Postgraduate Institute of Science, University of Peradeniya, Peradeniya, Sri Lanka.
[2] Department of Chemistry, University of Peradeniya, Peradeniya, Sri Lanka.

Contact Information of the corresponding author
Email: namalpriyantha@pdn.ac.lk
Telephone: +94812394445
To whom correspondence should be addressed

Abstract

The value addition of the peel of the edible fruit of *Artocarpus nobilis*, a plant endemic to Sri Lanka, performed through treatment with 0.010 M NaOH solution leads to the high removal of Cr(VI) and Cr(III) demonstrating its superior nature as a biosorbent. Owing to the fact that this waste material of a locally available edible fruit employed in the biosorption process makes it low-cost, environmentally friendly and energy efficient, which are of great advantages when compared to chemical treatment procedures practiced at present. The static experiments conducted using synthetic solutions of Cr(VI) and Cr(III) ions with NaOH-modified peel of *Artocarpus nobilis* fruit (NWBF) lead to the optimum parameters of 0.200 biosorbent dosage, 120 min shaking time and 30 min settling time. Regression analysis of linear and nonlinear fitting of adsorption data gathered through solution analysis after the suspension of NWBF and Cr species reaches equilibrium, followed by various error function determinations indicate that the Cr(III)/NWBF system follows Langmuir, Freundlich or Temkin isotherms, while the Cr(VI)/NWBF follows Freundlich and Sips isotherms. The monolayer adsorption capacities (q_{max}) determined through nonlinear curve fitting are 52.90 mg g^{-1} and 14.39 mg g^{-1} for Cr(VI) and Cr(III), respectively. Adsorption characteristics of NWFB are complicated due to non-homogeneous characteristics which lead to less precise results compared to those of homogeneous surfaces.

Keywords: *Artocarpus nobilis,* isotherm, optimization, error functions, linear, non-linear

1. Introduction

Purification of wastewater to fulfill the requirements of quality parameters depending on the type of consumption has become a necessity to maintain environment sustainability. Although many methods have been in operation, adsorption, owing to unique advantages, has become attractive in wastewater purification through the removal of toxic pollutants (Braket 2011; Priyantha et al. 2015a). An effective adsorbent, especially for large-scale or industrial-scale treatment, should possess many desirable characteristics, such as low-cost, ready availability, environmental friendliness, efficient mass transfer and chemisorption ability (Brakat 2011; Joseph et al. 2019). Adsorption is a specific interaction between the adsorbent and adsorbate; therefore, it would not be possible to have a general adsorbent for environmental pollutants having different chemical characteristics. Nevertheless, several materials have demonstrated their superior ability as adsorbents, in particular, for the removal of heavy metals abd dyes from industrial effluents. They include clay minerals, activated carbon and synthetic materials (Weng et al. 2008; Brakat 2011, Priyantha et al. 2015b; Joseph et al. 2019). These adsorbents have preferential affinity toward a particular group of environmental pollutants thereby offering selectivity of the removal process to some extent.

It has become a novel trend to use biomaterials, such as agricultural waste and byproducts or waste from large-scale industrial operations (Wang et al. 2009). These biosorbents offer many advantages, such as high efficiency, low-cost and possibility of regeneration. Many biosorbents have been tested for their ability of removing heavy meal ions from contaminated solutions; tea waste for Cu(II), Ni(II) and Zn(II) (Thakur and Parmar, 2013), coffee waste for Cr(VI), Cu(II) and Ni(II) (Pujol et al. 2013), rice husk for Cd(II), Cr(III), Cu(II), Ni(II), Pb(II) and Zn(II) (Priyantha et al. 2015a), eggs shell for Cr(III) and Cr(VI) (Daraei et al. 2014; Elabbas et al. 2016), breadfruit peel for Ni(II) (Priyantha and Kotabewatta, 2019; Kotabewatta et al., 2020) and Jackfruit peel for Ni(II) and Cr(III) (Ranasinghe et al. 2018). More importantly, improvement of the efficiency of removal and enhancement of selectivity can be made by chemical processing and/or surface modification of the biosorbent through which the mode of chemical interaction could be altered to strengthen the affinity toward chemical species. Moreover, both equilibrium and kinetics aspects, which could be independent of each other, should be considered for sound understanding of the adsorption process (Dissanayake et al. 2016).

Adsorption systems can be characterized by investigating the amount of the adsorbate adsorbed as a function of equilibrium concentration of the adsorbate in solution (Priyantha et al. 2015a; Priyantha et al. 2015b). In many instances, the extent of adsorption is indirectly determined by analyzing the adsorbate phase for the unabsorbed amount after the establishment of equilibrium (Lim et al. 2014). If the amount of adsorbate transferred to the adsorbent phase is more than what is required for a monolayer, it may be predicted that adsorption isotherms such as Freundlich and Sips which support multilayer adsorption be favored (Dissanayake et al. 2016). Nevertheless, it would not be possible to form an adsorbed layer of a metal on another metallic layer; *i.e*., multilayer formation of metals. Instead, what would be possible is to have different modes of mass transfer, such as transfer to macropores, mesopores and micropores through intra-particle and inter-particle diffusion, and surface complexation (Zhe et al. 2013). Therefore, unlike the mass transfer on orderly surfaces for which adsorption isotherms would directly be able to interpret experimental results, natural biosorption systems are so complex that direct application of theory would mislead what would really happen at molecular level. This aspect should thus be thoroughly understood although due attention has not been paid. This situation is more complex when the biosorbent surface is modified, as the modification process would introduce more variables.

The main objective of this study is to fill the above void by investigation of biosorption characteristics of a cationic and an anionic metallic species, namely Cr(III) and Cr(VI), at the state adsorption equilibrium, through fitting into various adsorption isotherm systems in their linear and nonlinear forms using peel of NaOH-modified *Artocarpus nobilis* fruit (NWBF) as the biosorbent. Although 0.01 M NaOH modified biosorbent (NWBF) has been recently reported (Samaraweera et al. 2020) for its ability to remove heavy metals, equilibrium aspects have not been addressed in detail (Zhe et al. 2013). Such investigation would be helpful to understand different modes of mass transfer, thereby extension of adsorption equilibrium data for the design of large-scale treatment systems to remove heavy metal ions from industrial effluents in environmentally friendly and economical manner would be feasible. Chromium species was specifically selected for this investigation because the contamination of the environment with chromium species has become a public health issue due to industrial emissions by metal finishing industries, iron and steel foundries, inorganic chemical plants, and tanneries. Moreover, in aqueous systems, although chromium is present in Cr(III) and Cr(VI) oxidation states, the latter is well-known to be highly toxic and carcinogenic to mammals, including humans. It can also cause allergic reactions, respiratory disorders, weaken the immune system, and kidney, liver and gastric damage (Kratochvil et al. 1998; Arris et al. 2014; Song et al. 2016; Lee et al. 2017).

2. Materials and Methods

2.1 Sample Preparation, Materials and Instrumentation

Matured *Artocarpus nobilis* (Wild breadfruit - WBF) fruits were randomly collected from Kandy District, Sri Lanka, washed with tap water, and peeled off. The peel was again washed with distilled water, air-dried, and ground to obtain particles of 0.710 mm < d < 1.00 mm. The samples were treated with acid (HNO_3 or CH_3COOH), base (NaOH), complexing agent (EDTA) and salt (NaCl) allowing 1.0 h stirring and 24 h settling. Thereafter, treated biosorbent samples were again washed with tap water followed by distilled water until the pH of washings was equal to that of water used for washing. The samples thus prepared were stored dry under ambient conditions for further experiments. The blank sample was prepared using the same conditions and treated with distilled water.

Analytical grade $K_2Cr_2O_7$ and $Cr_2(SO_4)_3.6H_2O$ were used to prepare standard solutions in distilled water. Analytical grade HNO_3, HCl, CH_3COOH, NaOH and NaCl were used for modification of WBF. The pH was adjusted using analytical grade 0.1 M NaOH and/or 0.1 M HNO_3. The total Cr concentration in solution was determined using Thermo M series atomic absorption spectrophotometer (AAS). Scientific pH meter (Orion Model 960) was used for pH measurements, scanning electron microscope (SEM) (Oxford Instruments Model ZEISS EVO|LS15)was used to record SEM images and X-ray Fluorescence (XRF) spectrometer (Fischerscope Model DF500FG-456) was used to record XRF spectra.

2.2 Optimization of parameters and batch studies

Selected experimental parameters, namely, biosorbent dosage, shaking time and settling time, were optimized for efficient removal of Cr(VI) and Cr(III) species using NWBF biosorbent at 150 rpm agitation speed when needed. For optimization of dosage, an aliquot of 50.0 mL of 10.00 mg L^{-1} of Cr(III)/Cr(VI) was shaken with NWBF by changing mass from 0.020 g to 0.300 g maintaining 1.0 h shaking time and 1.0 h settling time. By keeping the optimized biosorbent dosage fixed, shaking time was optimized by employing different shaking times from 0 to 180 min at 1.0 h settling time. Optimized biosorbent dosage and optimized shaking time were then kept fixed, and settling time (waiting time) was optimized. The ambient solution pH of 5.0 for Cr(III) and 2.0 for Cr(VI) was used without any alteration, and the concentration of NaOH solution used for surface modification of the biosorbent was used as 0.010 M (Samaraweera et al. 2020). The removal efficiency was calculated as per Equation (1),

$$\text{Removal percentage} = \frac{C_0 - C_f}{C_0} \times 100 \qquad (1)$$

where C_0 and C_f are initial and final concentrations, respectively, of Cr(III)/Cr(VI) in solution phase.

Under the optimum conditions, adsorption experiments were carried out for different concentrations up to 330 mg L^{-1} for Cr(III) and up to 2000 mg L^{-1} for Cr(VI). The mass of metal ions adsorbed per unit mass of the biosorbent is calculated as per Equation (2),

$$q_e = \frac{(C_0 - C_f)V}{m} \qquad (2)$$

where q_e is metal uptake (mg kg^{-1}) and V (L) and m (kg) are solution volume and mass of the adsorbent, respectively.

3. Results and Discussion

3.1 XRF investigation of NWBF biosorbent

Figure 1 shows the XRF spectrum of NWBF biosorbent before and after adsorption of Cr(III) and Cr(VI) which indicates that the biosorbent contains mainly K and Ca elements. According to the spectra, both Cr(III) and Cr(VI) are present on the surface of the biosorbent after treatment, and further, Cr(III) is more strongly adsorbed as compared to Cr(IV).

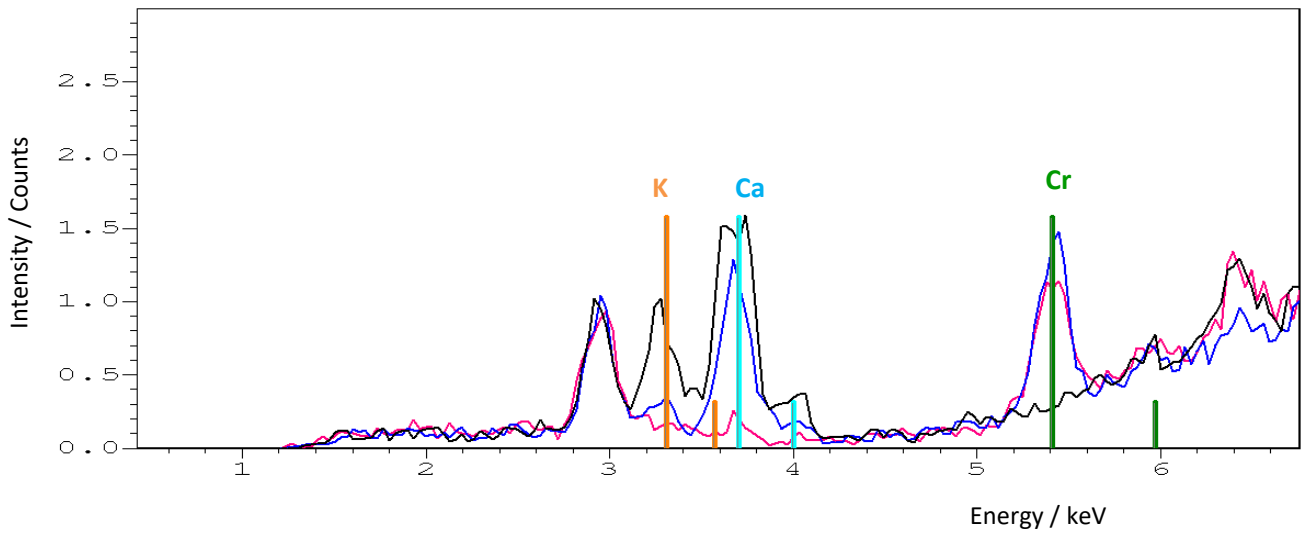

Figure 1: XRF spectrum of powdered NWBF: before adsorption (___), after Cr(VI) adsorption (_____) and after Cr(III) adsorption (_____). Lines indicate the specific peak locations of respective elements.

3.2 Surface titrations of NWBF biosorbent

The surface charge is an important characteristic of amphoteric colloids and suspensions. Surface charge in such systems depends on activities of potential-determining ions, mainly H^+ and OH^-, and the ionic strength of the medium. The surface charge density thus depends on $[H^+]$ and $[OH^-]$, and it is usually calculated using Equation (3),

$$\text{Charge density} = \frac{F}{a \times s}\{(C_a - C_b) - [H^+] + [OH^-]\} \quad (3)$$

where F is the Faraday constant, a is the specific surface area (1.2×10^3 m^2 g^{-1}) (Kotabewatte et al. 2019), s is the composition of NWBF biosorbent particles in the suspension, $[H^+]$ and $[OH^-]$ are the equilibrium concentrations of hydronium and hydroxyl ions, C_a is the initial acid concentration, and C_b is the initial base concentration. Depending on the surrounding pH, adsorbent surface can be negative, positive or having no charge. The pH at which the net total particle charge is zero is called the isoelectric point (IEP) (Tran et al. 2017). If the surrounding pH is above its IEP, the adsorbent surface bears a net negative charge, showing its ability to exchange cations, and vice versa. The IEP for NWBF determined using surface charge density - medium pH curves constructed in $NaNO_3$ solutions of three different ionic strengths is 4.1, based on the point of intersection of the three curves (Figure 2).

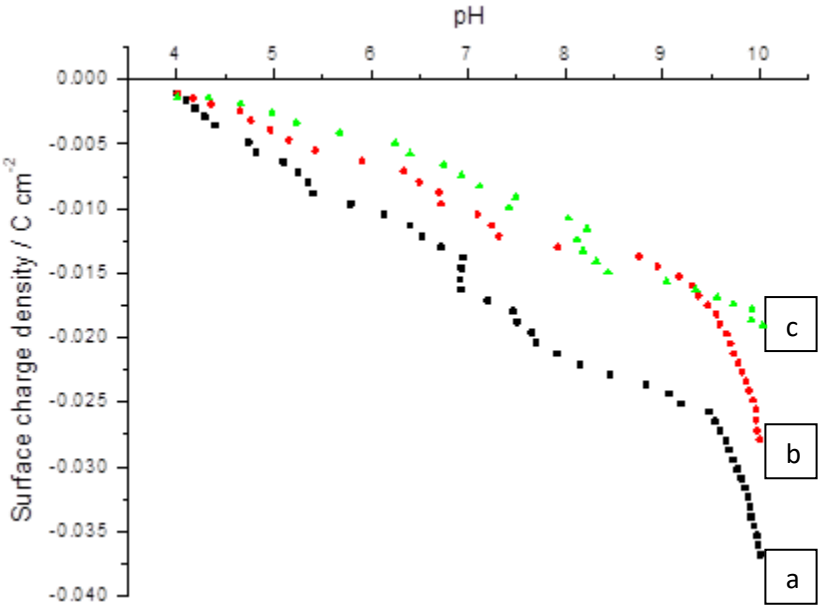

Figure 2: Variation of surface charge density vs. pH for NWBF biosorbent in $NaNO_3$ solutions of (a) 0.001 M, (b) 0.010 M and (c) 0.10 M.

3.3 SEM images of NWBF biosorbent

SEM images give the details of morphological features and surface characteristics of the biosorbent material. The SEM images of the NWBF biosorbent before and after exposure to Cr species are shown in Figure 3, which indicates the surface coverage after exposure. NWBF, being a porous material having pores of different sizes, contributes to high surface area leading to efficient biosorption [Figure 3(a)]. Also, variable-sized pores contribute to intraparticle

diffusion. After biosorption, Cr species would diffuse into pores in addition to the surface coverage leading to the loss of Cr(III)/Cr(VI) species from solution equivalent to more than a monolayer although multilayer formation is unlikely.

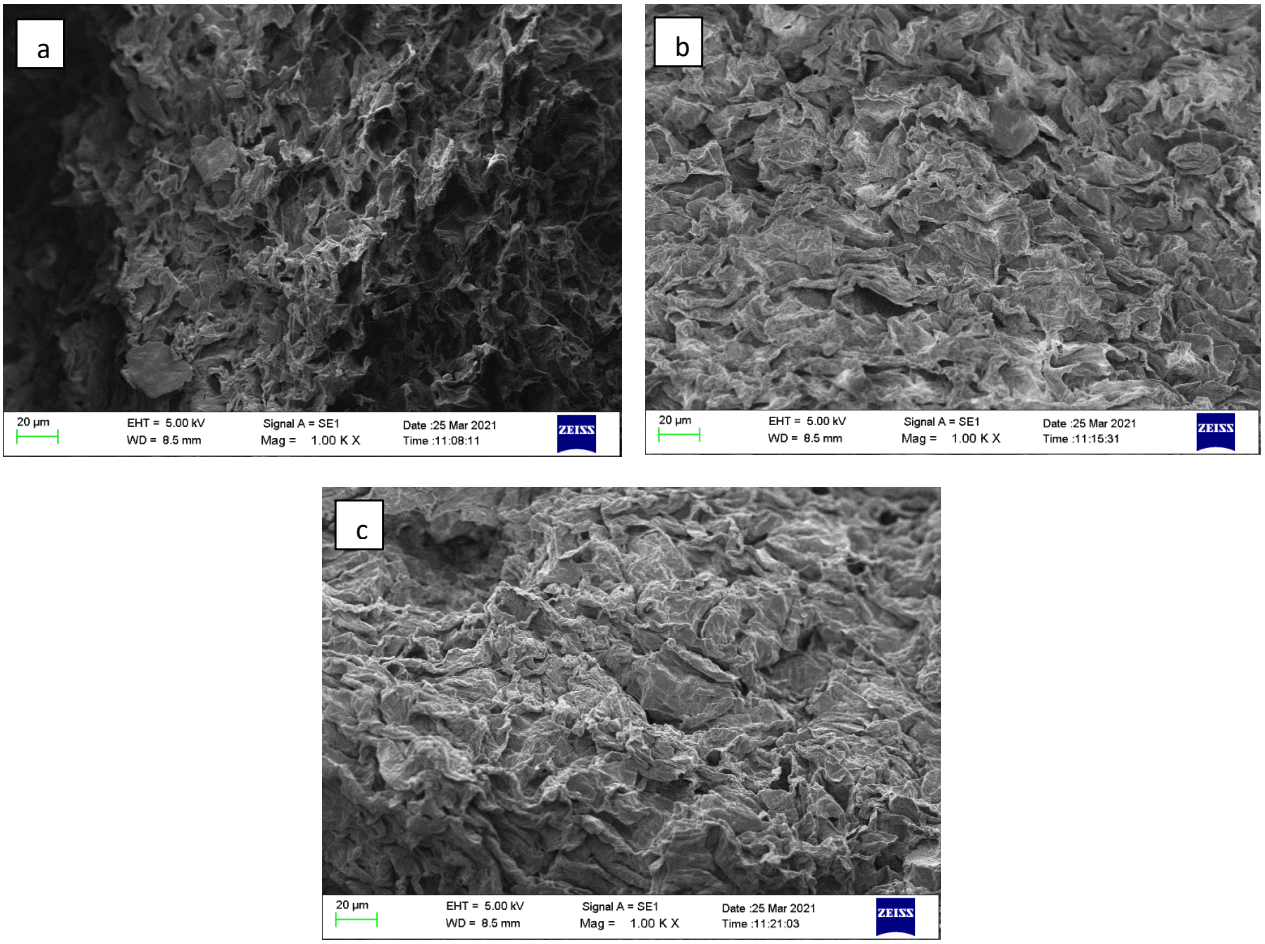

Figure 3: The SEM images at 1000 magnification for (a) NWBF biosorbent, (b) Cr(III) adsorbed NWBF biosorbent and Cr(VI) adsorbed NWBF biosorbent.

3.4 Selection of a suitable agent for modification of WBF

Variation of the extent of removal with different modified agents is shown in Figure 4. Accordingly, acid-treated WBF shows a lower extent of removal of Cr(III) as compared to that of the blank. The extent of removal comparatively increases upon treatment of WBF with the base, NaOH and the salt, NaCl. These observations conclude that the surface of WBF is positive and that positively charged Cr(III) cannot be attached to the surface more efficiently at pH 5.0. On the other hand, negatively charged Cr(VI) ions can attach to the surface of both acid and base treated WBF at pH 2.0. The NaCl-treated WBF shows an increased extent of removal compared to the bank. Thus, ion exchange may take place in salt-treated WBF. Consequently, NaOH-treated WBF was taken for further experiments because NaOH modified WBF shows high removal of both Cr(III) and Cr(VI). Although there is no significant increase in the extent of removal after NaOH modification, long-term stability of the chemically treated biosorbent, which is due to the protection of the surface, is a great advantage of modification, which is required for large-scale industrial applications.

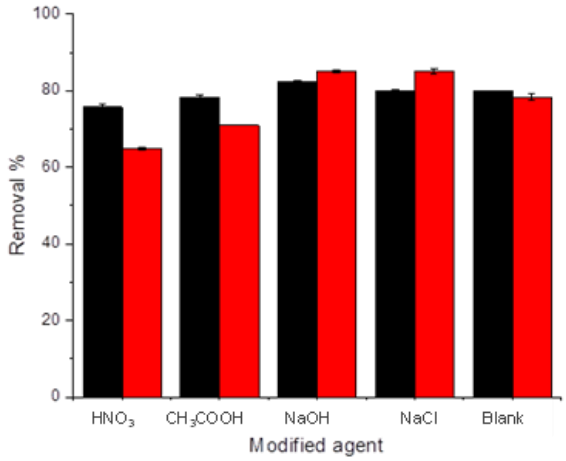

Figure 4: Extent of removal of Cr(III) (red) and Cr(VI) (black) from 10 ppm solutions after modifying the biosorbent with each reagent at 0.1 M concentration [pH 2.0 for Cr(VI) and pH 5.0 for Cr(III), 2.0 h shaking, 20 min settling and 0.200 g of biosorbent].

3.5 Effect of biosorbent dosage, shaking time, settling time and pH on extent of Cr removal

As expected, the extents of removal of both Cr(III) and Cr(VI) were increased with an increase in the dosage of the biosorbent [Fig 5(a)]. Although the extent of removal is not completely levelled off, biosorbent mass of 0.200 g was selected as optimum for both Cr species considering the compromise between the extent of removal and the biosorbent dosage. The effect of variation of shaking time on the extent of removal with the optimized biosorbent dosage is shown in Figure 5(b). The extent of removal of both Cr(III) and Cr(VI) is increased with shaking time reaching the maximum after 100 min with small variations thereafter. Therefore, the shaking time of 120 min was selected as optimum for both species. Thereafter, the extent of removal of Cr(III) and Cr(VI) investigated at the optimum dosage and at the optimum shaking time shows that it is independent of the settling time [Figure 5(c)]. However, a settling time of 20 min was considered as optimum at which it can be assured that the biosorbent-adsorbate system has reached equilibrium.

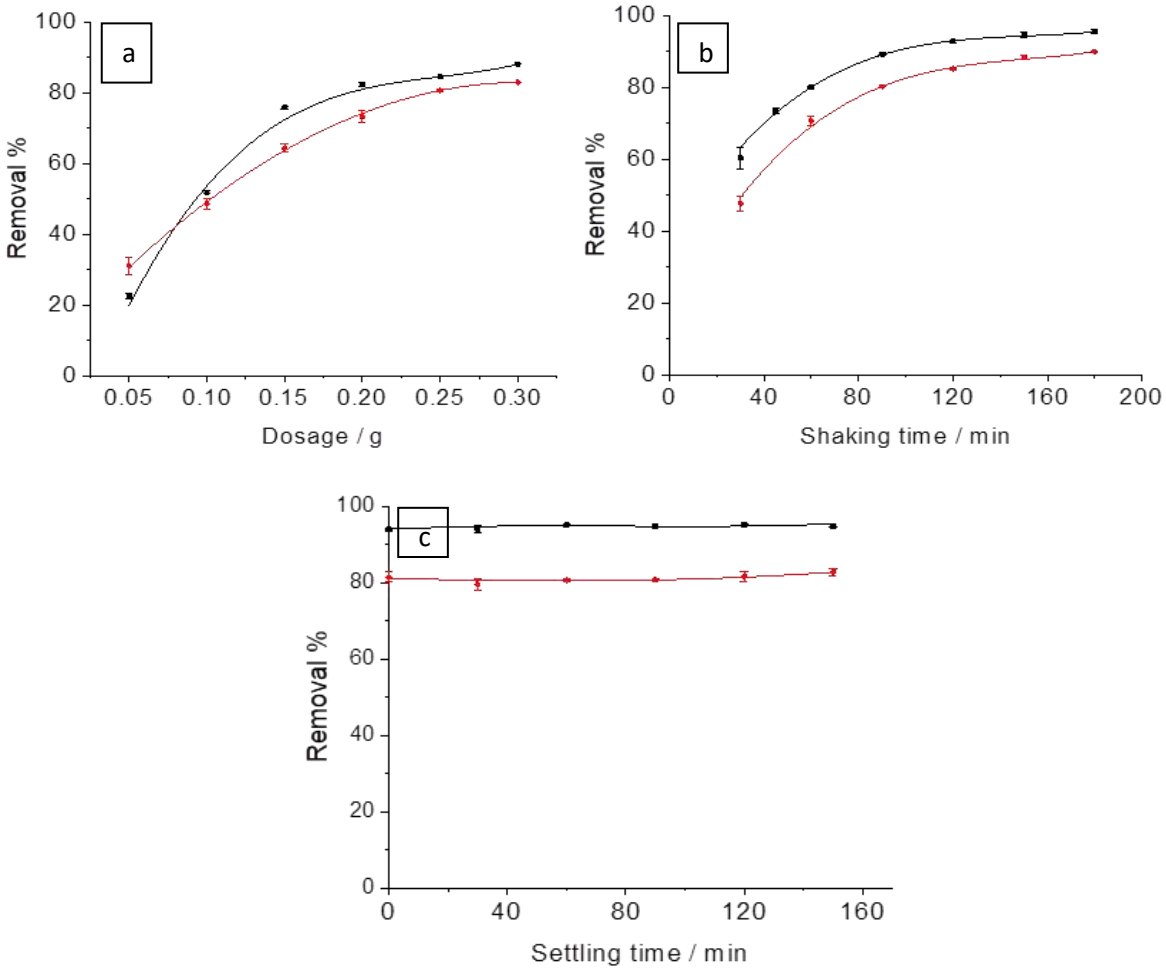

Figure 5: Variation of extent of removal with (a) dosage, (b) shaking time and (c) settling time [50.0 mL of 10.0 mg L^{-1} concentration of Cr solutions treated with NWBF, Cr(III) (●) and Cr(VI) (●)].

3.6 Adsorption isotherms and error analysis

The distribution of metal ions between the solution and the biosorbent phase at constant temperature can be expressed by two-parameter and three-parameter isotherm models. To obtain the best-fitted adsorption isotherm model, the mass of adsorbate adsorbed (q_e) can be plotted against equilibrium concentration (C_e) as per the linearized and non-linearized equations of each model (Table 1). Figure 6 shows that the variation of q_e vs. C_e of Cr(III) and Cr(VI) under the optimum conditions (biosorbent dosage, shaking and settling time and pH) and non-linear fittings of the isotherm models. The pH adjustment of adsorbate is necessary to do the experiments under optimum conditions. Although NaOH is added to the biosorbent-adsorbate suspension for pH adjustment, Cr(III) precipitates as $Cr(OH)_3$ when ionic concentration reaches above the value determined from its solubility product. Therefore, the maximum initial concentration of Cr(III) was taken as 330 mg L^{-1} at pH 5.0 in isotherm studies. However, Cr(VI) does not show precipitate formation within the range of pH investigated, which is an advantage for Cr(VI) studies.

Figure 6 provides a clear indication on biosorption of Cr(III) and Cr(VI) onto the surface of NWBF. The Cr(III)/NWBF system follows Type I(b) while the Cr(VI)/NWBF system follows Type IV(b) diverse shape as per IUPAC isotherm classification. The behaviour of Type I(b) suggests that NWBF have wider micropores and possible narrow mesopores, and Type IV(b) also gives evidence for the presence of mesopores on NWBF (Thommes et al. 2015).

Equilibrium data are important for designing a biosorption system to contribute to building an adsorption mechanism. Thus, data were further analyzed using five different isotherm models, namely Langmuir, Freundlich, Temkin, Dubinin–Raduskevich (D-R) and Langmuir–Freundlich isotherm (Sips model) (Table 1). The most suitable model is identified using non-linear and linear regression analysis, and error functions determination.

Table 1: Non-linear and linearized equations of isotherm models used for analyzing data

Name of the isotherm	Non-linear form	Linear form
Langmuir	$q_e = \frac{q_{max} K_L C_e}{1 + K_L C_e}$	$\frac{C_e}{q_e} = \frac{1}{q_{max}} C_e + \frac{1}{K_L q_{max}}$
Freundlich	$q_e = K_F C_e^n$	$\ln q_e = \ln K_F + n \ln C_e$
Temkin	$q_e = \frac{RT}{b_T} ln K_T C_e$	$q_e = \frac{RT}{b_T} \ln K_T + \frac{RT}{b_T} \ln C_e$
D-R model	$q_e = q_{DR} \exp\{-K_{DR}\varepsilon^2\}$ $\varepsilon = RT \ln\left(1 + \frac{1}{C_e}\right)$ $E = \frac{1}{\sqrt{2K_{DR}}}$	$\ln q_e = \ln q_{DR} - K_{DR}\varepsilon^2$
Sips model	$q_e = \frac{q_m K_s {C_e}^{1/n}}{K_s {C_e}^{1/n} + 1}$	$\ln\left(\frac{q_e}{q_m - q_e}\right) = \frac{1}{n} \ln C_e + \ln K_s$

q_{max} (mg kg^{-1}) = maximum saturated monolayer adsorption capacity of an adsorbent; C_e (mg L^{-1}) = adsorbate concentration at equilibrium; q_e (mg kg^{-1}) = amount of adsorbate uptake at equilibrium; K_L (L mg^{-1}) = constant related to the affinity between an adsorbent and adsorbate; K_F (mg$^{(1-n)}$ kg^{-1} L^{-n}) = Freundlich constant; n (dimensionless) = Freundlich intensity parameter, which indicates the magnitude of the adsorption driving force or the surface heterogeneity; q_{RD} (mg kg^{-1}) = adsorption capacity; K_{RD} (mol^2 J^{-2}) = constant related to the sorption energy; E (J mol^{-1}) = mean adsorption energy; R = gas constant, T = temperature in Kelvin; q_m (mg kg^{-1}) = maximum adsorption capacity; Ks = Sips constant; $1/n$ = Sips model exponent.

The Langmuir isotherm model describes that the biosorbent material has uniformly distributed energetically equivalent sites, and monolayer biosorption takes place on the surface of the biosorbent. The Langmuir model states that a limited number of ions can sorb on the surface, and after saturation, no further adsorption occurs. On other hand, the Freundlich isotherm model describes that the biosorption takes place in heterogeneous surface with uneven distribution of the ions on the biosorbent surface and it is accounted with multilayer adsorption. The D-R isotherm model was developed to account for the mean biosorption free energy from which the prediction of adsorption type is available and the Temkin isotherm is used to describe the effect of temperature. The Sips model is the combination of the Langmuir and Freundlich models which follows the Langmuir at high adsorbate concentrations, while at low

concentration, it tends toward the Freundlich model (Khamwichit et al. 2022). The isotherms stated above, Langmuir, Freundlich, Temkin and D-R models are two-parameter isotherms, while the Sips model is a three-parameter isotherm.

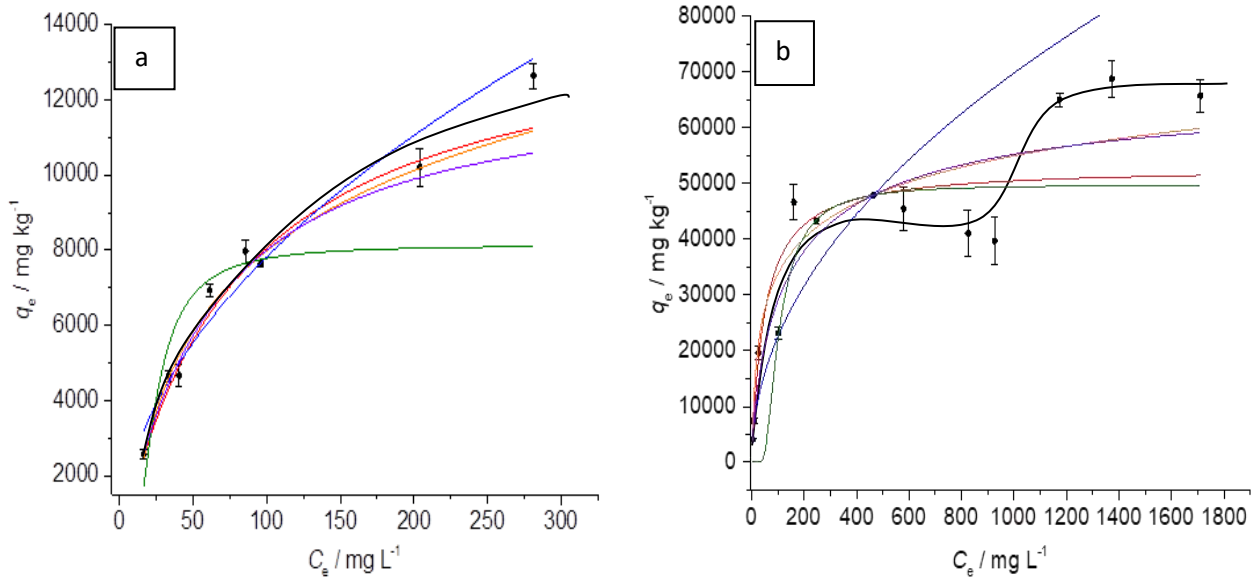

Fig 6: Nonlinear fittings of **e**xperimental data (▬) of variation of amount of Cr adsorbed vs. initial concentration of (a) Cr(III) and (b) Cr(VI) and the Langmuir (▬), Freundlich (▬), Temkin (▬), D-R (▬) and Sips (▬) [50.0 mL of 10.0 mg L^{-1} concentration of metal ion solutions, 0.200 g dosage, 120 min shaking time, 30 min settling time, 300.15 K temperature, pH = 2.0 for Cr(VI) and pH = 5.0 for Cr(III) treated with NWBF]

The linear forms of the adsorption isotherm relationships are given in Figure 7. The regression analysis can be performed using Equation (3) to determine the coefficient of determination (R^2). The strength of the relationship between the dependent and independent variables can be predicted using the R^2 value, which ranges from 0 to 1, with values close to 1 showing a good fit.

$$R^2 = (\text{correlation coefficient}, r)^2 = \frac{S_{xy}}{S_x S_y} \qquad (3)$$

where $S_{xy} = \frac{\sum x_i y_i - \frac{\sum x_i \sum y_i}{n}}{n-1}$, S_x is standard deviation of x's, S_y is standard deviation of y's, x is independent variable and y is dependent variable.

The parameters of linear and non-linear regression analysis determined for each isotherm model are given in Table 2. The linear and non-linear parameter values are much similar for both Cr(III)/NWBF and Cr(VI)/NWBF systems. The R^2 values of linear forms of the Cr(III)/NWBF and Cr(VI)/NWBF systems decrease in the order, Sips > Langmuir > Temkin > Freundlich > D-R and Freundlich > Langmuir > Temkin > Sips> D-R, respectively. Accordingly, the best linear fitted model is the Sips isotherm for Cr(III)/NWBF system and the Freundlich isotherm for Cr(VI)/NWBF system. The Freundlich parameter, *n,* for Cr(III) /NWBF and Cr(VI)/NWBF systems spread between 0.40 – 0.52. The

value of the *n* parameter gives information on the heterogeneity of biosorbent sites: values of *n* significantly lower than 1 would reflect high heterogeneity (adsorption is a chemical process). The biosorbent contains -OH, -COH, -COOC- and Ph-OH groups (Kotabewate et al. 2019). Thus, the adsorbate molecules attached to these functional groups and make chemical bonds.

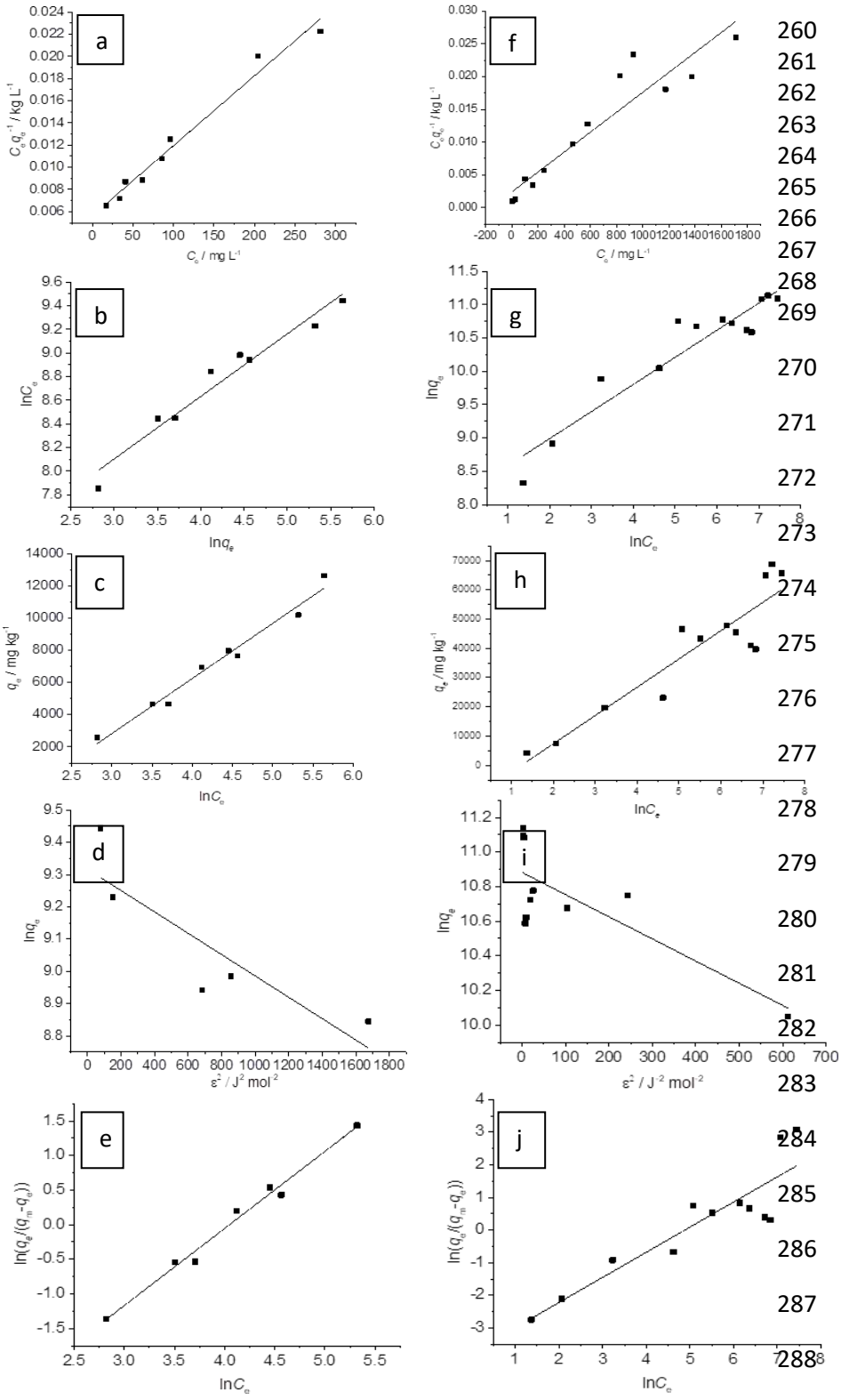

Figure 7: Linearized isotherm graphs for Cr(III)/NWBF system [(a) Langmuir, (b) Freundlich, (c) Temkin, (d) D–R model and (e) Sips model]; and Cr(VI)/NWBF system [(f) Langmuir, (b) Freundlich, (c) Temkin, (d) D–R model and (e) Sips model].

Table 2: Parameters of isotherm models determined by experiment data

Model	Linear		Non-linear	
	Cr(III)	**Cr(VI)**	**Cr (III)**	**Cr(VI)**
Langmuir				
q_{max} (mg kg^{-1})	1.584×10^4	6.572×10^4	1.439×10^4	5.290×10^4
q_{max} (mg g^{-1})	15.84	65.72	14.39	52.90
K_L (mg L^{-1})	0.0111	0.0064	0.0127	0.0207
R^2	0.9783	0.8952	0.9689	0.9988
Freundlich				
K_F ($mg^{(1-n)}$ kg^{-1} L^{-n})	6.745×10^2	3.552×10^3	7.857×10^2	2.346×10^3
n	0.5298	0.4070	0.4990	0.4912
R^2	0.9565	**0.8990**	0.9655	0.9978
Temkin				
K_T (L mg^{-1})	0.1134	0.2894	0.1324	0.3960
b_T (J mol^{-1})	0.7282	0.2580	0.8077	0.2716
R^2	0.9761	0.8519	**0.9756**	0.9991
D-R model				
K_{DR} (J $mol^{-1})^{-2}$	0.0003	0.0013	7.3823	0.0013
q_{DR} (mg kg^{-1})	1.1122×10^4	5.3217×10^4	8.144×10^3	4.981×10^4
E (J mol^{-1})	38.87	19.76	0.26	19.61
R^2	0.7645	0.6074	0.8148	0.9841
Sips				
q_m (mg kg^{-1})	1.263×10^4	6.877×10^4	1.263×10^4	6.877×10^4
K_S $(L/mg)^{1/n}$	0.0109	0.0232	0.0131	0.0232
n	0.8966	1.2981	0.9429	1.3364
R^2	**0.9860**	0.8151	0.9620	**0.9994**

Adsorption behavior of an adsorbate can be further understood by evaluating different error functions, namely, Average relative error (ARE), Sum square error (SSE), Hybrid fractional error function (HYBRID), Sum of absolute error (EABS), Non-linear chi-square test (χ^2) and Marquardt's percent standard deviation (MPSD). The general equations for these error functions are given in Table 3. The main challenge of using SSE is that, at higher concentration, the squares of error increase. The MPSD error function is a modification of geometric mean distribution, and it is based on the number of degrees of freedom of a system. The HYBRID model is aimed to improve the applicability of the SSE at a lower concentration, and error function divided by the measured value and ARE function is used to get a meaningful idea of the accuracy of the experiment, arranging average of different absolute errors in order.

Table 3: Different error functions used in isotherm analysis.

Type of errors	Equations
ARE	$\frac{100}{n}\sum_{i=1}^{n}\left\lvert\frac{q_{e,meas}-q_{e,calc}}{q_{e,meas}}\right\rvert_i$
SSE	$\sum_{i=1}^{n}\left(q_{e,meas}-q_{e,calc}\right)_i^2$
HYBRID	$\frac{100}{n-p}\sum_{i=1}^{n}\left[\frac{\left(q_{e,meas}-q_{e,calc}\right)^2}{q_{e,meas}}\right]_i$
EABS	$\sum_{i=1}^{n}\lvert q_{e,meas}-q_{e,calc}\rvert$
χ^2	$\sum_{i=1}^{n}\frac{\left(q_{e,meas}-q_{e,calc}\right)^2}{q_{e,meas}}$
MPSD	$100\sqrt{\frac{1}{n-p}\sum_{i}^{n}\frac{\left(q_{e,meas}-q_{e,calc}\right)^2}{q_{e,meas}}}$

The error terms of both linear and non-linear isotherm models vary without any trend (Table 4). Both linear and non-linear forms of the Langmuir isotherm applied to the Cr(III)/NWBF system show low error values for HYBRID, MPSD and χ^2 functions; for the Cr(VI)/NWBF system, linear Sips model shows the smallest error for ARE function and non-linear Sips model shows the smallest error for MSPD and χ^2 functions. Considering both R^2 and error function values, it is argued that the Cr(III)/NWBF system follows the Langmuir, Freundlich or Temkin isotherms, while the Cr(VI)/NWBF follows the Freundlich or Sips isotherms.

Table 4: Error values of different adsorption isotherms.

	Error function	Langmuir	Freundlich	Temkin	D-R	Sips
Cr(III) Linear Model	ARE	5.72	8.56	6.63	96.50	**5.41**
	SSE	High	High	High	High	High
	HYBRID	**3631.40**	8026.52	4210.10	High	6152.58
	EABS	3366.74	4602.59	**3341.04**	High	3581.98
	MPSD	**6.98**	11.47	9.04	160.71	8.06
	χ^2	**217.88**	481.59	252.61	High	369.15

Cr(VI) Linear Model	ARE	26.62	20.40	19.20	36.36	**16.69**
	SSE	High	High	High	High	High
	HYBRID	High	High	High	High	High
	EABS	High	High	High	High	High
	MPSD	5162.54	4925.58	**4320.71**	6727.49	4388.83
	χ^2	29317.02	26687.45	**20535.43**	High	21188.06
Cr(III) Non-Linear Model	ARE	5.67	8.20	**5.43**	100	6.15
	SSE	High	High	High	High	High
	HYBRID	**4754.50**	7299.60	4909.47	High	7509.64
	EABS	3552.97	3797.18	**3285.74**	High	4144.49
	MPSD	**7.47**	12.04	9708.47	115.47	8.71
	χ^2	**285.27**	437.98	294.57	High	450.58
Cr(VI) Non-Linear Model	ARE	**15.89**	26.19	17.93	34.91	16.42
	SSE	High	High	High	High	High
	HYBRID	High	High	High	High	High
	EABS	High	High	High	High	High
	MPSD	4633.89	7306.66	4343.32	6791.06	**4237.58**
	χ^2	23620.21	58725.99	20750.90	High	**19752.80**

*High = Error Value > 3×10^4

3.7 Biosorption mechanism

The NWBF surface has various functional groups, such as carboxylic acids, esters and alcohol (Kotabewatte et al. 2019). The functional groups are deprotonated during the treatment with NaOH solutions becoming the surface of the biosorbent negatively charged. At the pH of 5.0, the Cr(III) ions are attached to these functional groups forming chemical bonds. However, at a pH of 2.0, $Cr_2O_7^{-2}$ ions are more likely to be reduced to Cr(III) with concomitant protonation of deprotonated functional groups (Saha et al. 2010). Thus, Cr(VI) ions mainly attach to the surface as Cr(III) ions. Figure 8 shows a graphical illustration of this process.

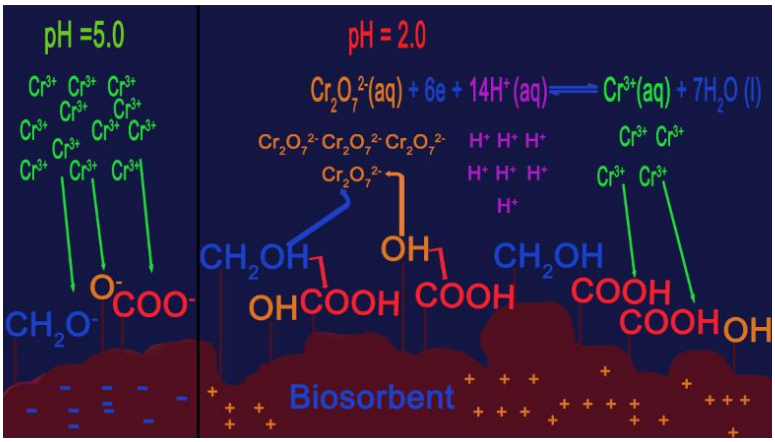

Figure 8: Biosorption mechanism for Cr(III) ions at 5.0 pH and Cr(VI) ions at 2.0 pH.

Conclusion

Peel of *Artocarpus nobilis* fruit modified with dilute sodium hydroxide solution (NWBF) behaves as an effective biosorbent for removal of both Cr(III) and Cr(VI) under optimum conditions leading to high monolayer adsorption capacities of 52.90 mg g^{-1} and 14.39 mg g^{-1} for Cr(VI) and Cr(III), respectively, based on non-linear curve fitting of the Langmuir adsorption isotherm. According to linear and non-linear regression analyses, and error function determinations, the Cr(III)/NWBF system follows Langmuir, Freundlich and Temkin isotherms while Cr(VI)/NWBF system follows Freundlich or Sips isotherms. Thus, monolayer formation would be extended to transfer of adsorbate species Cr(VI) and Cr(III) to micropores and mesopores possibly through intraparticle diffusion, which appears to be a multilayer process based on solution analysis. Moreover, Cr(VI) species available as $Cr_2O_7^{2-}$ would be reduced to Cr(III) by organic functionalities present in the biosorbent thereby improving the affinity toward biosorption. The present study demonstrates that NWBF has a great potential to be used as a low-cost adsorbent for removal of both Cr(III) and Cr(VI), two highly toxic species found in industrial effluents.

Acknowledgments

Special appreciation for the financial support provided by World Bank (Grant Number: 6026-LK/8743-LK) as well as for the immense support provided by the Postgraduate Institute of Science, University of Peradeniya, Peradeniya, Sri Lanka, and the Department of Chemistry, Faculty of Science, University of Peradeniya, Sri Lanka.

Author information

Authors and Affiliations

A.P.G.M.V. Samaraweera[1,2], N. Priyantha[2] and W.S.S. Gunathilake[2]

[1] Postgraduate Institute of Science, University of Peradeniya, Peradeniya, Sri Lanka.
[2] Department of Chemistry, University of Peradeniya, Peradeniya, Sri Lanka.

Contributions

Author N. Priyantha contributed to the conceptualization of the study, funding acquisition, investigation, and supervision. Data curation, data analysis, and writing the original draft of the manuscript were done by A.P.G.M.V. Samaraweera and W.S.S. Gunathilake. All authors contributed to reviewing and editing the manuscript.

Funding

This study was funded by the World Bank (Grant Number: 6026-LK/8743-LK).

Data Availability Statement

The data that support this study will be shared upon reasonable request to the corresponding author; Namal Priyantha. (namal.priyantha@yahoo.com).

Ethical approval

Not applicable. This research did not involve any human or animal subjects.

Consent for publication

All authors have given consent for the publication of the manuscript and the materials incorporated.

Competing interests

The authors declare that they have no conflict of interest.

References

Arris S, Lehocine MB (2014) Removal of hexavalent chromium from industrial wastewater by Cereal By-Product. 5th International Renewable Energy Congress (IREC), 1-6. https://doi.org/10.1109/IREC.2014.6826935

Brakat MA (2011) New trends in Removing heavy metals from industrial wastewater. Arabian Journal of Chemistry, 4:361-377. https://doi.org/10.1016/j.arabjc.2010.07.019

Daraei H, Mittal A, Mittal J, Kamali H (2014) Optimization of Cr (VI) Removal onto Biosorbent Eggshell Membrane: Experimental & Theoretical Approaches. Desalination and Water Treatment, 52(7-9):1307-1315. http://dx.doi.org/10.1080/19443994.2013.787374

Dissanayake DMREA, Wijesinghe WMKEH, Iqbal SS, Priyantha N, Iqbal MCM (2016) Isotherm and kinetic study on Ni(II) and Pb(II) biosorption by the fern Asplenium nidus L. Ecological Engineering, 88:237-241. https://doi.org/10.1016/j.ecoleng.2015.12.028

Elabbas S, Mandi L, Berrekhis F, Pon MN (2016) Removal of Cr (III) from chrome tanning wastewater by adsorption using two natural carbonaceous materials: eggshell and powdered marble. Journal of Environmental Management, 166:589-595. https://doi.org/10.1016/j.jenvman.2015.11.012

Joseph L, Jun B, Flora JRV, Min C, Yoon Y (2019) Chemosphere removal of heavy metals from water sources in the developing world using low-cost materials: A review. Chemosphere, 229:142–159. https://doi.org/10.1016/j.chemosphere.2019.04.198

Khamwichit A, Dechapanya W, Dechapanya W (2022) Adsorption kinetics and isotherms of binary metal ion aqueous solution using untreated venus shell. Heliyon, 8(6). https://doi.org/10.1016/j.heliyon.2022.e09610

Kotabewatta PA, Priyantha N (2019) Biosorption of heavy metal ions on peel of Artocarpus nobilis fruit: 1 — Ni (II) sorption under static and dynamic conditions, Applied Water Science 9:37. https://doi.org/10.1007/s13201-019-0911-2

Kotabewatta PA, Priyantha, N and Lim LBL (2020) Biosorption of heavy metal ions on peel of *Artocarpus nobilis* fruit: 2. Improvement of biosorption capacities of Ni (II) through different modifications, Desalination and water treatment 185, 226-236.

Kratochvil D, Pimentel P (1998) Removal of Trivalent and hexavalent chromium by seaweed biosorbent, 32 (18), 2693–2698.

Lee CG, Lee S, Park JA, Park C, Lee SJ, Kim SB, An B, Yun ST, Lee SH, Choi JW (2017) Removal of copper, nickel and chromium mixtures from metal plating wastewater by adsorption with modified carbon foam. Chemosphere, 166:203–211. https://doi.org/10.1016/j.chemosphere.2016.09.093

Lim LBL, Priyantha N, Ramli UK, Ing CH (2014) Adsorption of Cd(II) ions using Lamiding, a wild vegetable from Brunei Darussalam. Journal of Applied Phytotechnology in Environmental Sanitation, 3(2): 65- 74.

Priyantha N, Navaratne AN, Kulasooriya TP (2015a) Adsorption of heavy metal ions on rice husk: isotherm modeling and error analysis. International Journal of Earth Science and Engineering, 8(2):346-352. http://dx.doi.org/10.4038/jnsfsr.v46i2.8413

406 Priyantha N, Lim LBL, Wickramasooriya S (2015b) Adsorption behavior of Cr(VI) by Muthurajawela peat.
407 Desalination and Water Treatment, 1-9. http://dx.doi.org/10.1080/19443994.2015.1081835

408 Priyantha N and Kotabewatta PA (2019) Biosorption of heavy metal ions on peel of *Artocarpus nobilis* fruit: 1—
409 Ni(II) sorption under static and dynamic conditions, Applied Water Science 9, 1-10

410 Pujol D, Bartrolí M, Fiol N, Torre FDL (2013) Modelling synergistic sorption of Cr (VI), Cu (II) and Ni (II) onto
411 exhausted coffee wastes from binary mixtures Cr (VI)–Cu (II) and Cr (VI)–Ni (II). Chemical Engineering, 230:396-
412 405. https://doi.org/10.1016/j.cej.2013.06.033

413 Ranasinghe SH, Navaratne AN, Priyantha N (2018) Enhancement of adsorption characteristics of Cr(III) and Ni(II)
414 by surface modification of jackfruit peel biosorbent. Journal of Environmental Chemical Engineering, 6(5):5670-
415 5682. https://doi.org/10.1016/j.jece.2018.08.058

416 Saha B, Orvig C (2010) Biosorbents for hexavalent chromium elimination from industrial and municipal effluent.
417 Coordination Chemistry Reviews, 254:2959-2972. https://doi.org/10.1016/j.ccr.2010.06.005
418
419 Samaraweera APGMV, Priyantha N, Gunathilake WSS, Kotabewatta PA, Kulasooriya TPK, (2020), Biosorption of
420 Cr(III) and Cr(VI) species on NaOH modified peel of *Artocarpus nobilis* fruit. 1. Investigation of kinetics. Applied
421 Water Science 10:115. https://doi.org/10.1007/s13201-020-01187-2
422
423 Song D, Pan K, Tariq A, Azizullah A, Sun F (2016) Adsorptive removal of toxic chromium from waste-water using
424 wheat straw and *Eupatorium adenophorum*. PLoS ONE 11(12). https://doi.org/10.1371/journal.pone.0167037

425 Thakur LS and Parmar M (2013) Adsorption on heavy metal (Cu^{2+}, Ni^{2+} and Zn^{2+}) from synthetic wastewater by tea
426 waste adsorbent. International Journal of Chemical and Physical Sciences 2(6): 6-19.

427 Thommes M, Kaneko K, Neimark AV, Olivier JP, Rodriguez-Reinoso F, Rouquerol J, Sing KSW (2015)
428 Physisorption of gases, with special reference to the evaluation of surface area and pore size distribution (IUPAC
429 Technical Report) 87(9-10):1051-1069. https://doi.org/10.1515/pac-2014-1117
430
431 Tran HN, You SJ, Bandegharaei AH, Chao HP (2017) Mistakes and inconsistencies regarding
432 adsorption of contaminants from aqueous solutions: A critical review. Water Research 120:88-116.
433 http://dx.doi.org/10.1016/j.watres.2017.04.014
434
435 Wang J, Chen C (2009) Biosorbents for heavy metals removal and their future. Biotechnol. Advance, 27(2):195–226.
436 https://doi.org/10.1016/j.biotechadv.2008.11.002

437 Weng CH, Sharma YC, Chu SH (2008) Adsorption of Cr(VI) from Aqueous solutions by spent activated clay. Journal
438 of Hazardous Materials, 155:65-75. https://doi.org/10.1016/j.jhazmat.2007.11.029

439 Zhe XU, Jian-guo CAI, Bing-cai PAN (2013) Mathematically modeling fixed-bed adsorption in aqueous systems,
440 Journal of Zhejiang University-Science, 14(3):155-176. https://doi.org/10.1631/jzus.A1300029

Supplementary Files

This is a list of supplementary files associated with this preprint. Click to download.

- GA.tiff